Journal of Advanced Marine Engineering and Technology, Vol. 50, No. 1, pp. 24~36, 2026
J. Advanced Marine Engineering and Technology (JAMET)
https://doi.org/10.5916/jamet.2026.50.1.24

ISSN 2234-7925 (Print)
ISSN 2765-4796 (Online)
Original Paper

Development and verification of idealized structural unit members for efficient strength assessment of LNG cargo tank scaffolding

Jung Kwan Seo† · Dae Kyum Park[1] · Simkwan Oh[2] · Joo Shin Park[3]

(Received January 22, 2026 ; Revised February 6, 2026 ; Accepted February 22, 2026)

Abstract: This study proposes an efficient structural assessment methodology for scaffolding systems installed inside LNG cargo tanks, which function as essential temporary structures during insulation installation and construction. Conventional design relies on experience-based modeling and 3D beam finite element (FE) analyses, which require considerable effort and often overestimate stiffness under combined loading. To address these limitations, an Idealized Structural Unit Member (ISUM) approach is introduced, replacing complex multi-component scaffolding members with equivalent 1D beam elements having idealized sectional properties. These properties are derived through inverse calibration using axial buckling and bending responses from nonlinear 3D shell FE analyses. Validation is performed through unit-member analyses under various boundary and loading conditions, as well as partial system-level models representing actual LNG tank configurations. Results show that the ISUM model predicts critical buckling loads with less than 1% error compared to experiments and detailed models. Under combined loading, it produces up to 20% lower stresses than conventional 3D beam models, while vertical displacement differences remain within 1 mm. The findings demonstrate that the ISUM approach reduces modeling complexity and computational demand while maintaining accuracy, offering a practical method for the design and safety verification of LNG tank scaffolding.

Keywords: System Scaffolding, LNG Carrier Cargo Tank, Idealized Structural Unit Member, Strength Assessment

1. Introduction

During the construction of LNG carriers, various internal temporary structures are required inside cargo holds to support insulation installation and structural support activities. Among them, system scaffolding plays a critical role as a temporary structure by enabling material transportation, worker accessibility, and safe working conditions. Such scaffolding systems are assembled into temporary tower-type structures composed of multiple steel unit members connected through pins, bolts, and hinges. Although these structures are temporary in nature, their structural safety must satisfy stringent criteria. In particular, the recent trend toward larger and more geometrically complex cargo holds has increased the demand for more rigorous and reliable structural design and verification methods.

Previous studies on scaffolding systems have primarily focused on improving construction and installation methods in shipyard environments **[1]-[3]**. However, these studies do not provide detailed procedures or methodologies for structural safety assessment under actual insulation installation conditions, nor do they establish systematic frameworks for the development of new scaffolding systems. Moreover, inconsistencies in evaluation methods and criteria highlight the need for regulatory analysis and the establishment of unified assessment frameworks.

Research related to scaffolding design and standards includes studies on alternative temporary scaffolding for power plant maintenance **[4]**, the development of high-strength scaffolding structures and materials **[5][6]**, and investigations into load combinations based on design standards **[7]**. In addition, numerous studies have addressed structural analysis using equivalent stiffness elements and simplified finite element models **[8][9]**, mainly focusing on complex structures such as truss systems, steel-framed buildings, and sandwich panels for strength and

† Corresponding Author (ORCID: http://orcid.org/0000-0002-3721-2432): Professor, Department of Naval Architecture and Ocean Engineering/The Korea Ship and Offshore Research Institute, Pusan National University, 2, Busandaehak-ro 63beon-gil, Geumjeong-gu, Busan, 46241, Rep. of KOREA, E-mail: seojk@pusan.ac.kr, Tel: +82-51-510-2415

1 Research Professor, The Korea Ship and Offshore Research Institute, Pusan National University, E-mail: daekyeom@pusan.ac.kr

2 Pro, Ship and Offshore Research Institutes, Samsung Heavy Industries, E-mail: simkwan.oh@samsung.com

3 Group Manager, Ship and Offshore Research Institutes, Samsung Heavy Industries, E-mail: scv7076@nate.com

vibration assessment.

More recently, a previous study **[10]** proposed a simplified analysis approach based on idealized structural elements for rapid structural evaluation at the conceptual design stage of LNG cargo hold scaffolding systems. While this approach demonstrated notable improvements in modeling efficiency and computational time, its sectional properties were defined primarily based on equivalent stiffness concepts, limiting its ability to accurately capture unit-member buckling behavior and structural responses under combined loading conditions. Furthermore, quantitative verification of stiffness overestimation inherent in conventional one-dimensional beam models remained limited.

To date, the design and verification of scaffolding systems still rely heavily on empirical knowledge and simplified finite element models, resulting in repetitive and time-consuming design–verification cycles and an increased risk of human error. Looking ahead, the introduction of next-generation cargo containment systems for hydrogen and ammonia carriers will further intensify the need for automated and highly reliable structural verification methods capable of accommodating diverse geometries and structural characteristics.

Therefore, this study advances previous research by introducing an Idealized Structural Unit Member (ISUM) approach, in which sectional properties are inversely derived based on three-dimensional shell finite element analyses and experimental results at the unit-member level. The proposed methodology is systematically extended and validated at both partial and system levels, thereby providing a more realistic and reliable structural assessment framework for LNG cargo hold scaffolding systems.

2. Scaffolding System of LNG Cargo Tank

The scaffolding system used for the construction of LNG cargo tanks is composed of various main structural members and auxiliary structural members, as illustrated in **Figure 1**. The main unit members include columns, girders, braces, brackets, and big trusses, while the auxiliary members consist of legs, joint frames, and other connecting components. In the initial structural design stage, all main and auxiliary members are modeled using detailed three-dimensional (3D) beam finite element models to evaluate the structural performance of the scaffolding system.

In this study, among the various components of the scaffolding system, four representative column types and eighteen girder types—commonly used in LNG cargo hold scaffolding at shipyards—were selected, as summarized in **Table 1**. The representative

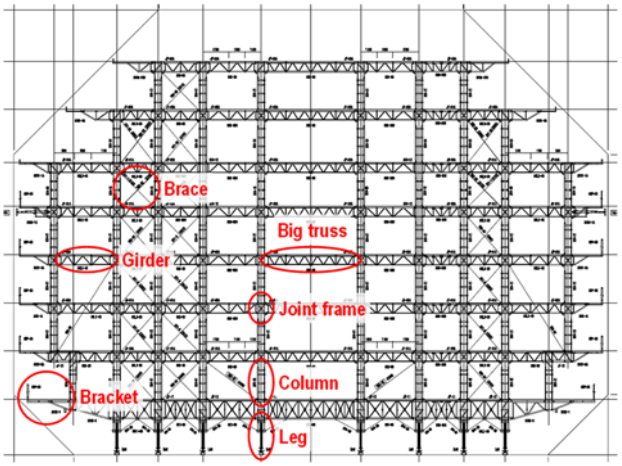

Figure 1: A Typical LNG cargo tanks scaffolding system

Table 1: Typical geometry of the scaffolding system

Model Type	Sectional shape	Chord (mm)	Materials	Length (mm)
C4	Circular	60.5x2.4	STK540	1,797~2,602
G1	Circular	48.6x2.4	STK540	2,020
G2	quadrilateral	50x50x2.3	STKR490	2,184
G3~G13	Circular	48.6x2.4	STK540	2,020~6,000
G14~G18	quadrilateral	50x50x3.2	STKR490	2,260~6,000

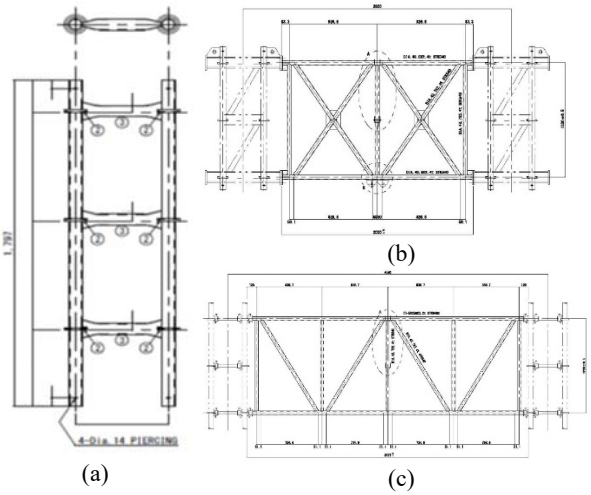

Figure 2: A Typical column and girder unit member: (a) C1, (b) G3, and (c) G8 of the scaffolding system

geometries of Column C1 and Girder G8 are illustrated in **Figure 2**. Columns C1 through C4 correspond to the primary column-type members, while G1 through G18 represent girder members with diverse cross-sectional configurations. The main dimensions of the column members consist of circular sections with lengths ranging from 1,797 mm (C1) to 2,602 mm (C4). The girder members typically employ circular or rectangular cross-sections and are connected using pins, bolts, or hinge mechanisms, with lengths varying from

Table 2: Material characteristics of scaffolding system

Material	Min. yield strength (MPa)	Tensile strength (MPa)	Reference standard
STK540	390	540	JIS G 3444
STKR490	325	490	JIS G 3466
SS400	245	400~510	JIS G 3101

approximately 2,020 mm (G1) to 6,000 mm (G18).

In this study, the connection characteristics of these members are not considered. Instead, the development and verification of the ISUM model focus on the beam- and girder-type unit members and the partial system composed of these primary and secondary structural components.

The scaffolding members are fabricated using structural carbon steels that comply with JIS standards **[11]**, such as STK540, STKR490, and SS400 as shown in **Table 2**. In the previous study on LNG cargo hold scaffolding systems, the loading conditions were categorized into uniformly distributed loads and horizontal/vertical concentrated loads applied to each member, reflecting the weights of various tools, materials, and workers during actual installation tasks. Accordingly, the loading conditions defined in the prior study **[10]** were adopted in the present analysis.

3. Application of Idealized Structural Members

3.1 Motivation for Simplified Structural Modeling

In current shipyard practice, FE models for structural analysis idealize each component of a unit member using 1D beam elements, and these assembled components form 3D beam-type unit members that constitute the full scaffolding FE model. As shown in **Figure 1**, even a single unit member requires dozens of elements with different sectional properties and material definitions. Consequently, the detailed geometry of each unit member must be implemented using 3D beam components, which significantly increases modeling complexity and computational effort.

The sub-members constituting each unit member are modeled as 1D beam or column elements with tubular (circular) or box/rectangular cross-sections. Their sectional properties are defined by geometric parameters such as outer diameter, wall thickness, width, height (or depth), and top/side wall thickness. Additional sectional properties, including axial area, torsional moment of inertia, and bending moments of inertia about the two principal axes, are also assigned. Based on the compressive and bending responses of these complex-shaped unit members, an idealized cross-sectional representation—referred to as the Idealized Structural Unit Member was developed. This approach

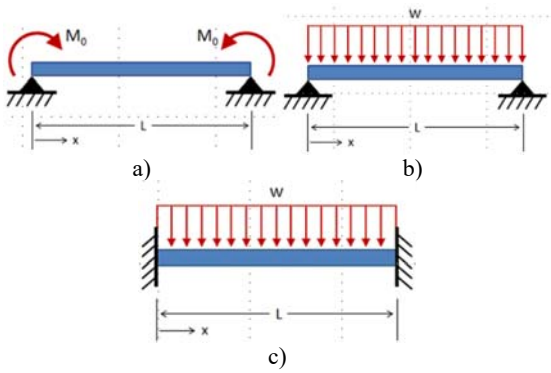

Figure 3: Boundary condition of bending behaviors

Table 3: Mathematical expression of varying boundary conditions under bending behavior of unit member

B.C.	S.S	S.S	Fixed	Unknown factors
Load	Moment	Distributed	Distributed	
Reaction (V)	-	$\frac{\omega L}{2}$	$\frac{\omega L}{2}$	V, ω
Moment ($M_{max.}$)	$M_{max.}$	$\frac{\omega L^2}{8}$	$\frac{\omega L^2}{12}$	$M_{max.}$, ω
Deflection ($\delta_{max.}$)	$\frac{M_{max.}L^2}{8EI}$	$\frac{5\omega L^4}{384EI}$	$\frac{\omega L^4}{384EI}$	$\delta_{max.}$, ω, I

enables equivalent sectional properties that capture the structural behavior of the original multi-component unit members to be incorporated into simplified FE models.

3.2 Mathematical Formulation for Idealized Unit Member

To develop the Idealized Structural Unit Member with an equivalent sectional representation, the first step is to determine the effective cross-sectional area (A). A based on the compressive behavior of the unit member. Using the relationship between axial load (P) and stress (σ = P/A), the effective area (A) can be obtained by relating the maximum compressive load (P_u) to the material yield strength (σ_Y).

For bending behavior, the dominant sectional property is the flexural stiffness (EI), and thus the effective moment of inertia (I) for bending unit members is evaluated. Considering the operational characteristics of the LNG cargo hold scaffolding system, the bending behavior is examined under relevant boundary conditions (simply supported and fixed–fixed) and load conditions (moment load and uniformly distributed load) as shown in **Figure 3.** The corresponding internal forces and displacements can be expressed using the analytical solutions of the linear elastic differential equation, as summarized in **Table 3**. By applying the relationship between the maximum deflection (δ_{max}), applied load, span length (L), and elastic modulus (E), the effective moment

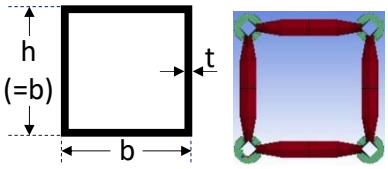

Figure 4: Square hollow section of column unit member

of inertia (I) can be inversely derived.

As shown in **Figure 4**, most unit members of the LNG cargo hold scaffolding system are composed of square hollow sections because the principal loading direction is clearly defined. Since the outermost fibers of these sections maintain a uniform shape with respect to the centroidal axis, their sectional properties can be expressed analytically.

Accordingly, the effective cross-sectional area (A) and moment of inertia (I) corresponding to the compressive and bending behaviors of the unit members are formulated as functions and solved numerically. The box-type unit members, illustrated in **Figure 4**, are idealized as square hollow sections, and their sectional properties (A and I) are expressed by **Equations (1)(2)**. By substituting the section width (b) with x and the wall thickness (t) with y, the three governing equations can be simplified into **Equations (3)(4)**. Solving these simplified equations yields the idealized sectional dimensions (b) and t for the ISUM formulation.

Although non-uniform unit members exhibit directionally varying stiffness characteristics, the ISUM formulation constructs the beam stiffness matrix using equivalent sectional properties that have been calibrated from 3D shell analysis results. These equivalent properties inherently incorporate the multi-directional stiffness contributions of the original member.

Once the effective sectional area and moments of inertia are obtained, the standard 6×6 beam stiffness matrix can be applied, as the equivalent section reproduces the global stiffness of the non-uniform member without explicit geometric modelling.

$$A = b^2 - (b-2t)^2,\ I = \frac{b^4-(b-2t)^4}{12} \tag{1}$$

$$b - 2t > 0 \tag{2}$$

$$x = \frac{(A+4y^2)}{4y},\ y = \frac{\pm\sqrt[4]{12\cdot I+x^4}-x}{2} \tag{3}$$

$$y < \frac{x}{2} \tag{4}$$

Thus, an idealized cross-section capable of faithfully representing the structural response of the actual member within its elastic range can be obtained.

3.3 Validation FE Modeling of Idealized Unit Member

Finite element modeling of the structural behavior of system scaffolding can be broadly classified into three approaches. The first approach, shown in **Figure 5(a)**, employs a 3D shell model in which all constituent components of a unit member—including hollow circular and square sections—are explicitly modeled using shell elements. This approach allows detailed prediction of local structural responses. The second approach (**Figure 5(b)**), represents the most commonly used modeling strategy, in which the overall three-dimensional geometry of the unit member is retained, while each detailed component is replaced by one-dimensional beam elements with equivalent sectional properties. This 3D beam unit member model provides relatively accurate results with reduced modeling effort. Finally, the third approach is the Idealized Structural Unit Method proposed in this study, in which the entire unit member is fully idealized using one-dimensional elements.

In this approach, the conventional models shown in **Figure 5(a)** and **Figure 5(b)** are replaced by a simplified 1D ISUM finite element model, as illustrated in **Figure 5(c)**.

To verify the applicability and accuracy of the proposed 1D ISUM model, comparative analyses were conducted using the commercial finite element code LS-DYNA **[12]** for the three modeling approaches shown in **Figure 5**. The target unit member selected for comparison is C1, a representative column-type member introduced in **Table 1**, which is used as both a column and a bending member in the system scaffolding.

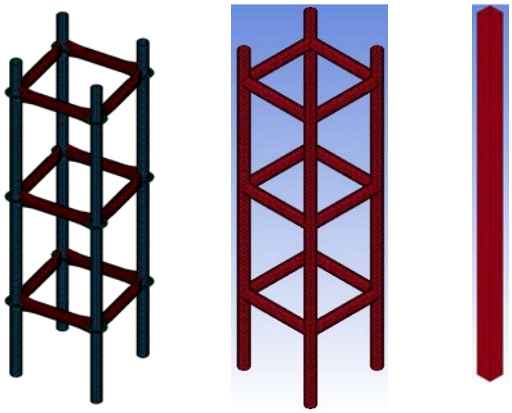

(a) 3D Shell model (b) 3D Beam model (c) 1D ISUM model

Figure 5: FE models for scaffolding column unit members

For non-uniform members such as G3 and G8, the structural contribution of internal braces is inherently reflected in the global load–deformation response obtained from the reference 3D shell analyses. The sectional properties derived from **Equations (1)** and **(2)** therefore represent equivalent stiffness parameters that reproduce the overall axial and bending behavior of the member, rather than direct geometric idealizations of the internal brace configuration.

Accordingly, **Equations (1)-(2)** can be applied to members with non-uniform geometry because the effective sectional area and moment of inertia are calibrated from the structural response of the detailed shell model rather than from the geometric dimensions of each component.

3.3.1 Reference FE Modelling

To assess the adequacy of the proposed 1D ISUM model, the three-dimensional (3D) shell model shown in **Figure 5(a)** was adopted as the reference model. To ensure the accuracy of the reference analysis, the shell element size was determined through a mesh convergence study. The convergence of bending behavior was examined by tracking the structural response for different mesh sizes. Specifically, the convergence was evaluated using the relationship between the applied bending moment and the maximum deflection under moment loading.

The slope of the linear region of the bending moment–maximum deflection curve, which corresponds to the bending stiffness, as well as the deflection at identical bending moments, were used as convergence indicators. Based on these criteria, the mesh convergence results were obtained and summarized in **Table 4**.

As the element size increased, the maximum deflection δ_{max} increased, while the corresponding bending stiffness decreased. Compared to the minimum element size, the maximum element size resulted in deviations of 12.52% in δ_{max} and −11.12% in bending stiffness. In addition, an identical convergence study was performed for the compressive buckling strength of the column-type unit member. In both cases, the influence of element size on the structural analysis results was clearly observed. Based on these findings, an element size of 5.0 mm was adopted for the 3D shell modeling, as it exhibited deviations of less than 0.32% in all evaluated metrics when compared with the results obtained using the minimum element size of 2.5 mm.

3.3.2 Column Type Unit Members

The compressive buckling behavior of four types of column-type unit members was investigated. The buckling characteristics were evaluated through a comparative analysis with existing

Table 4: Mesh convergence study results

s (mm)	Maximum deflection (δmax.)		Stiffness	
	(mm)	(%)	(kNm/mm)	(%)
2.5	2.38	-	41.95	-
5.0	2.38	0.05	41.92	-0.07
20.0	2.47	3.74	40.45	-3.57
40.0	2.68	12.52	37.29	-11.12

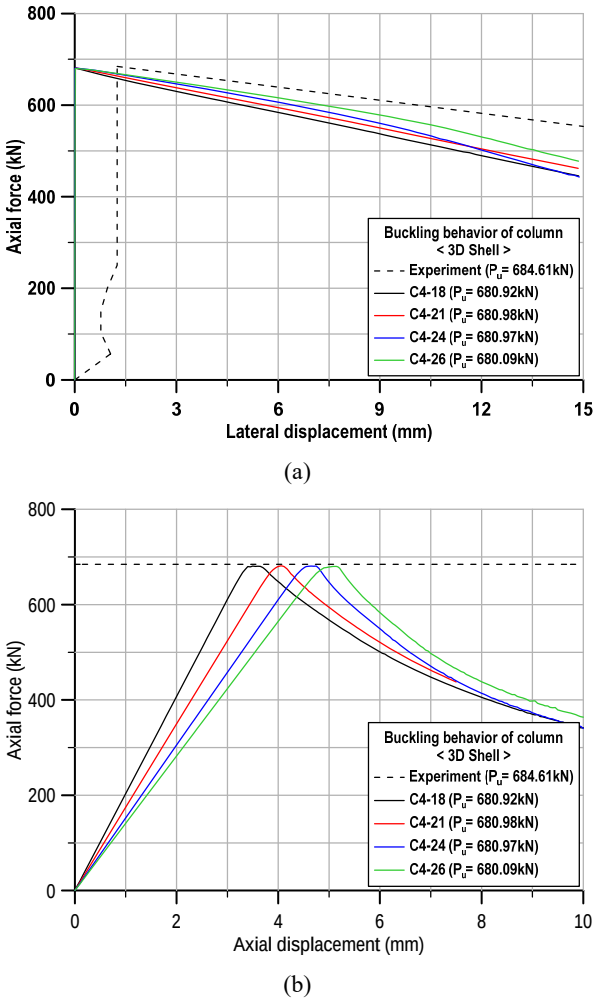

Figure 6: Results of axial force vs. displacement behaviors of 3D shell model: (a) lateral, (b) axial displacement

experimental results reported by Lee *et al.* **[2]**. **Figure 6(a)** presents the results of both the experimental tests and the nonlinear buckling analyses. In terms of the relationship between axial compressive load and lateral displacement, the experiments exhibited lateral deformations of approximately 2.0 mm up to the ultimate strength, whereas the numerical analyses showed only minor deformations of 0.11, 0.12, 0.07, and 0.12mm, respectively, at the ultimate load. The experimentally measured lateral displacements are larger than those predicted by the 3D shell analysis. This discrepancy primarily arises from the idealized

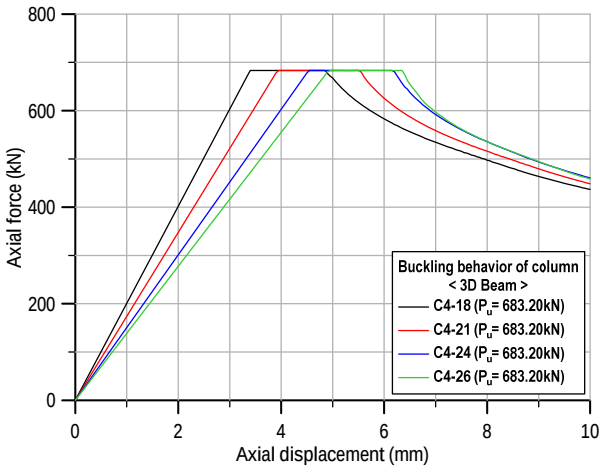

Figure 7: Results of axial force vs axial displacement behaviors of 3D beam model

assumptions inherent in the numerical model, including the absence of initial geometric imperfections, residual stresses, and uncertainties in boundary conditions.

In particular, the 3D shell model assumes a perfectly straight geometry, whereas the test specimens unavoidably contain initial out-of-straightness due to fabrication tolerances. Because column buckling behavior is highly sensitive to these imperfections, the experimental lateral displacements tend to increase more rapidly near the ultimate load.

Despite this difference in deformation magnitude, the numerical results predicted buckling strengths comparable to the experimentally observed maximum buckling load of 684.61kN.

Figure 6(b) illustrates the relationship between axial load and axial displacement. Consistent with the typical buckling behavior of column members with identical cross-sectional properties, a reduction in structural stiffness with respect to the buckling load was observed as the total member length increased. Overall, the results confirm very good agreement between the experimental data and the high-fidelity 3D shell modeling approach.

Figure 7 shows that the buckling strength obtained from the 3D beam modeling analysis is comparable to that predicted by the high-fidelity 3D shell model, with a value of 684.61kN. However, while the post-ultimate behavior observed in the 3D shell model reflects the material and geometric plasticity processes of the cross-section, the 3D beam model represents the member using a single beam cross-sectional property. As a result, a full-section plasticity behavior is exhibited after the ultimate load, which differs from the more detailed post-buckling response captured by the shell model.

In the present study, buckling analyses of the column-type unit

Table 5: Idealized section information for column unit member

Model	A (mm^2)	I (mm^4)		Idealized	
				(b)	(t)
C4-18	1,752	I_y	1,180,000	70.122	6.931
		I_z	34,100,000	343.011	1.282

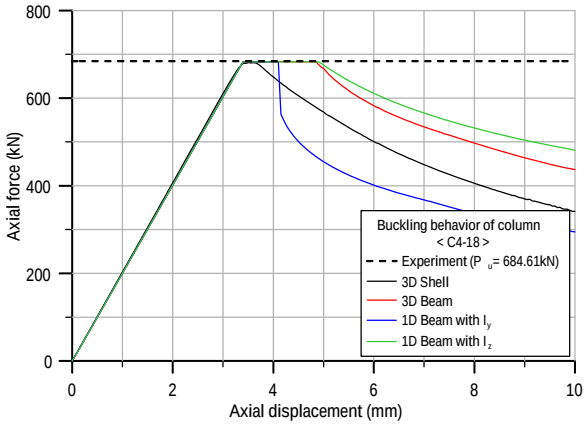

Figure 8: Results of axial force vs. displacement behaviors with varying models

members were conducted using 1D beam elements incorporating the idealized cross-sections derived from the proposed ISUM methodology. To examine the adequacy and behavioral fidelity of the idealized sectional properties, the cross-sectional parameters (A and I) reported in the previous study **[10]** were first adopted to construct the 1D beam model (see **Figure 5(c)**).

As shown in **Table 5**, the idealized square hollow section for the representative C4-18 member exhibits distinctly different width (b) and thickness (t) values because the axial moments of inertia vary, despite having the same nominal cross-sectional area.

The buckling analysis results for the C4-18 unit member, obtained using the 3D shell and 3D beam models as well as the idealized section based on the proposed ISUM approach, are presented in **Figure 8**. In terms of ultimate strength (P_u), all three models exhibited nearly identical values; however, notable differences were observed in their post-buckling responses.

The post-buckling responses differ among the modelling approaches due to the varying levels of geometric and material nonlinearities captured by each model. The 3D shell model accounts for local yielding, cross-sectional distortion, and geometric nonlinear effects such as ovalization, resulting in a gradual reduction in load-carrying capacity after buckling. In contrast, the conventional 3D beam model represents the member with a single

uniform beam section and cannot capture local shell effects.

Consequently, once the section reaches its yield limit, the beam model exhibits a rapid stiffness loss and abrupt post-buckling softening. For the ISUM models, the post-buckling trend varies depending on the adopted sectional moment of inertia, with larger inertia values delaying plasticization and producing a more gradual softening response. Since the ISUM formulation is designed to match the pre-buckling stiffness and ultimate capacity rather than detailed post-buckling behavior, some deviation in the softening region is expected.

In addition, the 1D beam models idealized using the axial moments of inertia about the y- and z-axes showed identical ultimate strengths but displayed distinct post-buckling behaviors, reflecting the sensitivity of plastic deformation progression to the selected principal moment of inertia. Although incorporating the axis-specific moment of inertia that best matches the 3D shell model's post-buckling trend may appear desirable, structural design practice generally evaluates member performance up to the yield or ultimate strength limits. Therefore, the cross-sectional area (*A*), rather than the moment of inertia (*I*), is identified as the dominant parameter governing buckling strength within the idealized framework.

In **Tables 6–8**, the 'Ratio (%)' denotes the relative difference between each numerical modelling approach and the reference model (experiment or 3D shell). For Table 6, the ratio expresses the percentage deviation of the predicted ultimate buckling strength from the experimental value. For Tables 7 and 8, the ratio quantifies the bending moment and maximum deflection compared to the 3D shell model, thereby identifying the relative structural stiffness overestimation in conventional 3D beam models and guiding the selection of conservative sectional properties for the ISUM formulation

Table 6 summarizes the buckling analysis results for all column-type unit members. While post-buckling characteristics varied among the models, both the ultimate strength P_u and the pre-buckling linear responses exhibited strong agreement across all analysis methods. The predicted P_u values differed from the experimental results by less than 0.66%, confirming that all numerical models provide reliable estimates of the buckling behavior. Based on the foregoing observations, the proposed 1D ISUM approach demonstrates that the axial load-carrying capacity is primarily governed by the effective cross-sectional area (*A*), and the effective area of each unit member was subsequently determined using **Equations (1)-(4)**.

Table 6: Buckling analysis results with experiment and FE models.

Model	Model type	$\delta_{max.}$ at P_u (mm)		P_u (kN)	Ratio (%)
C4-18 (Ref.)	Exp.	1.25	-	684.61	0.00
C4-18	3D Shell	0.11	3.50	680.92	-0.54
C4-21		0.12	4.10	680.98	-0.53
C4-24		0.07	4.75	680.97	-0.53
C4-26		0.12	5.10	680.09	-0.66
C4-18	3D Beam	-	3.40	683.20	-0.21
C4-21			3.95	683.20	-0.21
C4-24			4.55	683.20	-0.21
C4-26			4.95	683.20	-0.21
C4-18-I_y	1D Beam (ISUM)	-	3.40	683.20	-0.21
C4-18-I_z			3.40	683.00	-0.24
C4-21-I_y			4.00	683.20	-0.21
C4-21-I_z			4.00	683.40	-0.18
C4-24-I_y			4.55	683.20	-0.21
C4-24-I_z			4.55	683.40	-0.18
C4-26-I_y			4.95	683.20	-0.21
C4-26-I_z			4.90	680.40	-0.62

Table 7: Bending analysis results with FE models

Model	B+L	3D Shell		3D Beam		Ratio (%)	
		M_y	δ_{max}	M_y	δ_{max}	M_y	δ_{max}
C4-18	S.S + M	117.0	2.79	131.0	3.12	112	111
	S.S + ω	10.6	3.09	21.80	5.29	204	171
	F.C + ω	7.5	3.11	13.0	4.41	171	141
C4-21	S.S + M	116.1	3.80	131.0	4.06	112	106
	S.S + ω	10.6	3.21	24.74	5.87	232	183
	F.C + ω	7.2	3.04	16.2	5.25	223	172
C4-24	S.S + M	116.0	4.88	131.0	5.52	112	113
	S.S + ω	11.4	4.43	24.5	7.72	214	174
	F.C + ω	8.1	4.36	15.8	6.75	195	154
C4-26	S.S+ M	111.0	5.49	131.0	6.53	118	118
	S.S + ω	12.8	5.29	25.1	8.78	196	166
	F.C + ω	8.69	4.91	15.9	7.45	183	151

3.4.3 Girder Type Unit Members

The column-type unit members are primarily utilized as bending members during the installation process. Accordingly, bending analyses were performed for the girder-type unit members using both 3D shell and 3D beam models under two boundary

conditions, simply supported and fully fixed and two types of bending loads, namely moment loading and uniformly distributed loading. The analysis results within the linear range up to the first yield point were examined, and the bending moments and maximum deflections of the four representative bending-type members were compared for the two modeling approaches, as summarized in **Table 7**.

Although the 3D shell and 3D beam models exhibited generally similar bending behavior across all loading and boundary conditions, the 3D beam model consistently predicted higher bending stiffness than the 3D shell model. This indicates that the conventional 3D beam modeling approach tends to overestimate the bending strength of the unit members. Under uniformly distributed loading, which induces localized deformation due to the inherent non-uniformity of the cross-sections, the maximum deflection (δ_{max}) was evaluated as the primary indicator of bending behavior. At the onset of yielding, the bending moment predicted by the 3D beam model was approximately 112.0–232.1% higher, and the maximum deflection was 106.9–183.0% larger than those obtained from the 3D shell model.

The moments of inertia calculated for each loading condition represent the required sectional performance governing the bending behavior. To ensure structural safety through conservatism, the present study adopted the lowest moment of inertia obtained from the 3D shell bending analyses. Consequently, the moment of inertia corresponding to the fully fixed boundary condition with uniformly distributed loading for the C4-18 unit member was selected as the effective moment of inertia for the ISUM-based idealized beam model.

Similar to the column-type unit members, the effective moment of inertia (I) for the idealization of the bending-type unit members using the ISUM approach was evaluated based on the sectional properties presented in **Table 5**. **Table 8** summarizes

Table 8: Idealized section information for girder unit member

Model	b		t		I	
	mm	Ratio (%)	mm	Ratio (%)	mm^4	Ratio (%)
[10]	70.12	-	6.93	-	1,180,000	-
C4-18	76.27	8.8	6.25	-9.8	1,443,040	22.3
C4-21	89.22	27.2	5.21	-24.8	2,068,608	75.3
C4-24	88.68	26.5	5.25	-24.3	2,040,694	72.9
C4-26	91.57	30.6	5.06	-27.0	2,192,688	85.8

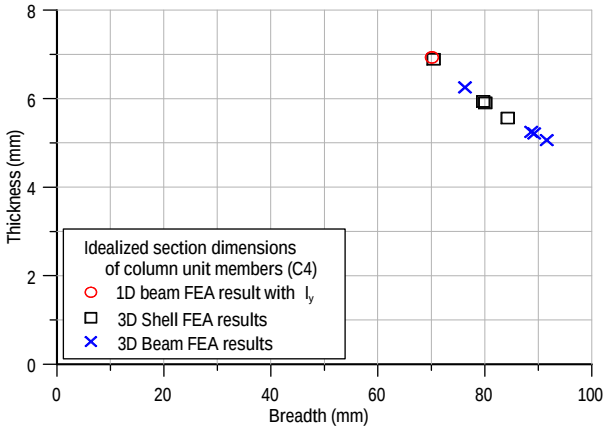

Figure 9: Idealized section dimensions of column unit members from FEA results.

the width (b), thickness (t), and moment of inertia (I) of the idealized sections, as well as their comparison with the results obtained from the 3D beam bending analyses. On the basis of the moment of inertia, the idealized ISUM sectional properties for members C-18, C-21, C-24, and C-26 can be regarded as conservative, corresponding to 22.3%, 75.5%, 72.9%, and 85.8% of the reference values, respectively.

4. Verification of Idealized Design Approach

4.1 Idealized Sections for Unit Column Member

The feasibility of developing an idealized square hollow section for the unit members used in the actual scaffolding system was examined through buckling and bending analyses, as well as the review of previous studies and the results presented in Section 3. For each unit member, the idealized sectional dimensions width (b) and thickness (t) were determined such that the structural responses under bending or compressive loading replicate those obtained from the reference 3D shell model. The resulting idealized sectional properties satisfied the cross-sectional area (A) and moment of inertia (I) values derived from the detailed analyses within a deviation of less than 0.05%, demonstrating strong agreement with both experimental data and prior studies.

Figure 9 presents a comparison of the derived idealized section dimensions (b and t). Although the sectional properties determined for each configuration accurately reflect the corresponding analysis results and are effective for reproducing the overall behavior, a single conservative idealized section was selected for application to the design of the full scaffolding system. Accordingly, the square hollow section with a width of 70.122 mm and a thickness of 6.937 mm derived from the area (A) and

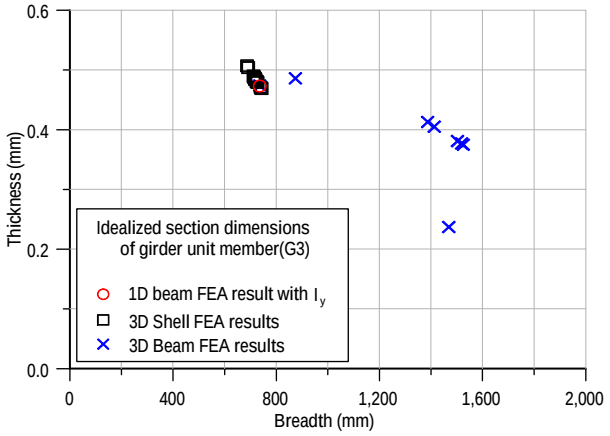

Figure 10: Idealized section dimensions of girder unit members from FEA results

the bending moment of inertia (Iy)was adopted as the final idealized sectional configuration.

4.2 Idealized Sections for Girder Unit Member

Using the same procedure applied to the compression-type unit members, a series of bending analyses was performed for the girder-type unit members to develop their idealized cross-sections. The resulting idealized sections, which adopt a square hollow configuration, satisfied the detailed analysis results in terms of both cross-sectional area (A) and moment of inertia (I) within a deviation of 0.09%.

Figure 10 presents the derived sectional dimensions, b and t, for the representative G3 member among the four sectional types considered. As in the case of the column-type unit members, the most conservative values among the required sectional properties were selected as the final idealized dimensions for the girder members.

Although the dominant structural mechanisms of column-type and girder-type unit members differ, buckling versus bending, the ISUM idealization procedure is equally applicable because both behaviors are governed by the effective sectional area (A) and moment of inertia (I) derived from the reference 3D shell and/or 3D Beam analysis.

For girder-type unit members, the effective moment of inertia was determined using the most conservative bending condition, namely the fixed–fixed boundary configuration subjected to uniformly distributed loading, ensuring that the bending-dominant behavior of the girder is properly accounted for. Thus, the identical idealization framework remains valid for both compression-type and bending-type unit members, as the equivalent sectional properties are calibrated directly from the structural responses of high-fidelity shell models.

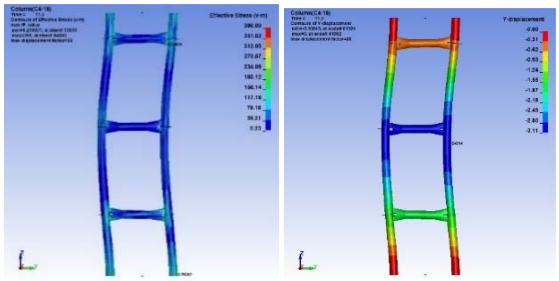

(a) 3D shell

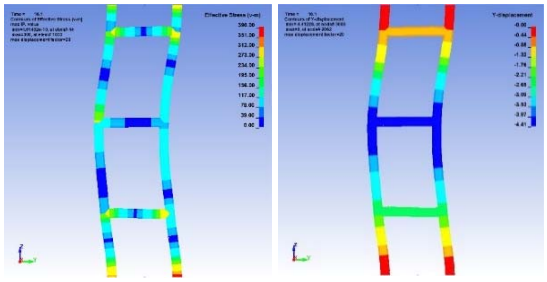

(b) 3D Beam

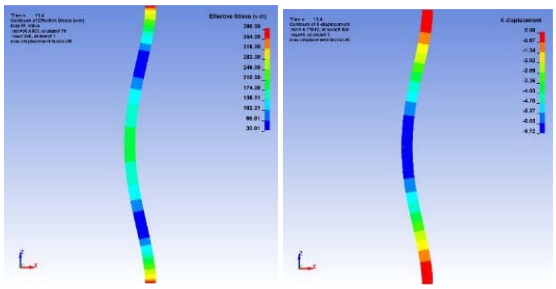

(c) 1D Beam

Figure 11: Bending analysis result under distributed loading on C4-18 unit member

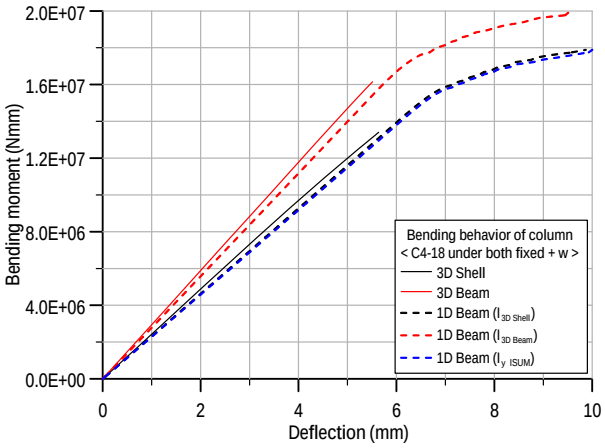

Figure 12: Bending behaviors of column unit members with 1D Beam models

4.3 Verification of Applicability for Unit Members

The applicability of the idealized sections was verified by comparing the ISUM-based 1D beam model with the 3D shell and 3D beam models in terms of displacement and stress responses for the column-type unit members. For the representative bending member C4-18, the bending behavior was illustrated in **Figure 11**, where the left panel shows the stress distribution and the right panel presents the displacement distribution for each modeling approach.

As shown in **Figure 12**, the deformation characteristics of the idealized 1D beam model exhibit behavior consistent with the analysis results of the 3D shell and 3D beam models, reflecting the corresponding moments of inertia (I) used in each case. However, minor differences were observed in the location and magnitude of the maximum deflection due to the inherent geometric asymmetry of the unit member along its longitudinal direction.

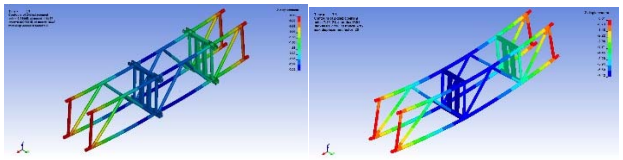

(a) 3D shell (b) 3D Beam

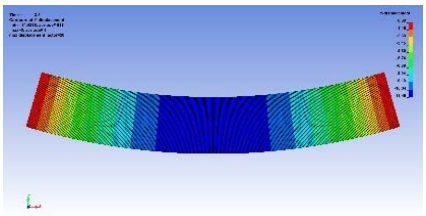

(c) 1D Beam

Figure 13: Bending analysis result under moment loading on an asymmetry girder, SG2-39 unit member

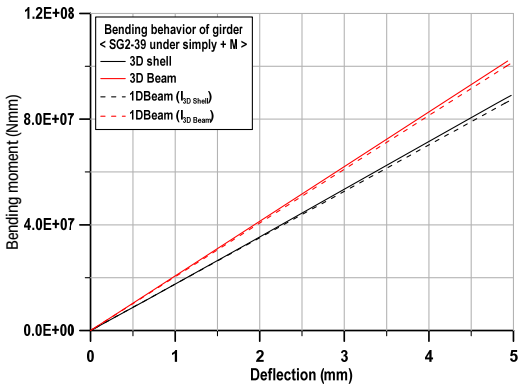

Figure 14: Bending behaviors of girder unit members with 1D Beam models on 4 different sectional signs

These observations confirm that the proposed ISUM-based 1D beam model provides an adequate and reliable representation of both the column and girder unit members. Accordingly, the sectional properties derived for the ISUM model using **Equations (1)-(4)**, based on either 3D shell or 3D beam analysis results, can be appropriately applied to the structural assessment of the scaffolding system.

4.4 Verification of Applicability to the Scaffolding System

4.4.1 Part Scaffolding System Modelling

To verify the practical applicability of the proposed ISUM-based 1D beam unit member model, comparative analyses were conducted between the ISUM model and the conventional 3D beam model widely used in shipyards. The selected part-model, illustrated in **Figure 15**, consists of column and girder unit members. In actual field applications, these unit members are connected and extended using joint frames to assemble the full scaffolding system. Accordingly, the connection modelling and boundary conditions were configured to closely replicate the installation environment of the LNG cargo tank.

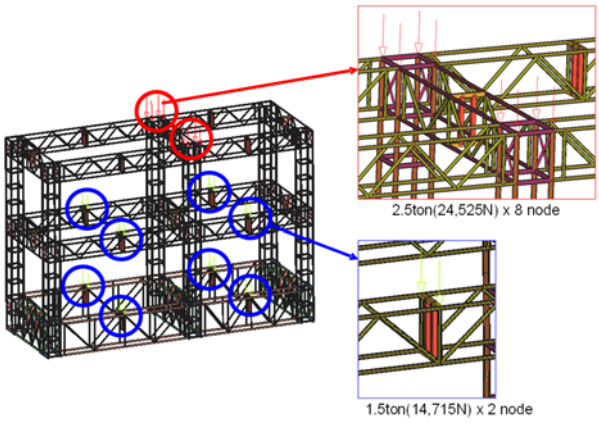

(a)

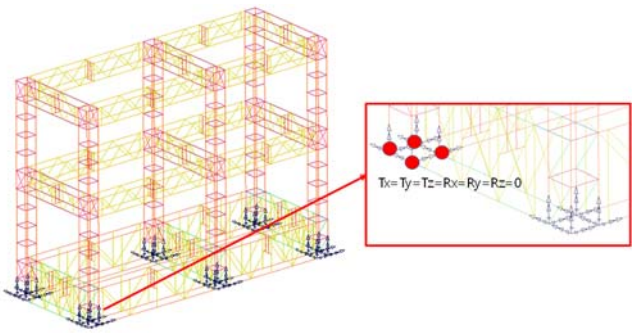

(b)

Figure 15: Loading and boundary condition of local model of system scaffolding for adaptability verification

Table 9: Applied the loading conditions

Loading case	Loading points	Total load (N)
Case I	Column + Girder	431,640
Case II	Column	196,200
Case II	Girder	235,440

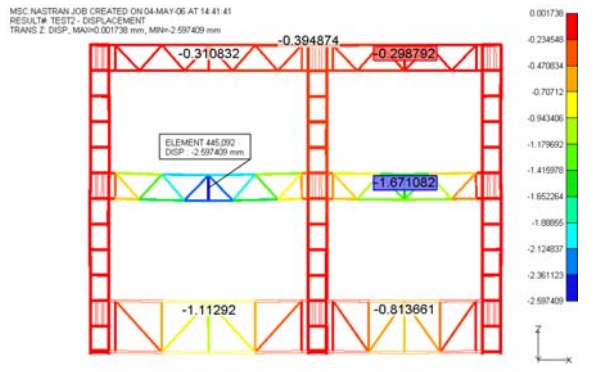

(a) 3D Beam model

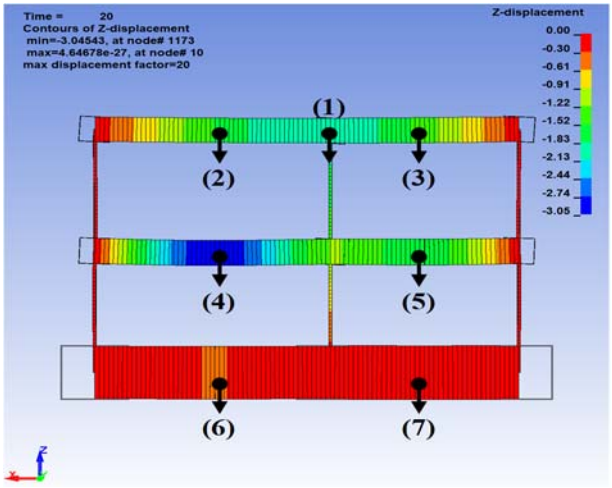

(b) ISUM model

Figure 16: Max. displacement and stress on scaffolding models: under loading Case I

The loading conditions were established based on those examined in previous studies **[10]**, distinguishing between combined loading conditions representative of actual working scenarios and single loading conditions. Representative loading scenarios used in the analysis are summarized in **Table 9**.

4.4.2 Comparison of Stress and Displacement Under Various Loading Conditions

Under the single loading conditions applied to the column-type unit member (Case II) and the independent loading applied to the girder-type unit member (Case III), the differences in maximum stress between the ISUM model and the conventional 3D beam model were only 0.92% and 2.81%, respectively. These results

Table 10: Comparison of maximum stress of the loading cases

Model / Case	3D Beam	ISUM	Difference	
	(MPa)	(MPa)	(MPa)	(%)
I	99.3	78.6	-20.70	-20.85
II	54.4	54.9	0.50	0.92
III	64.1	62.3	-1.80	-2.81

Table 11(a): Comparison of vertical displacements for Case I

Model / Location	3D Beam	ISUM	Difference	
	(mm)	(mm)	(mm)	(%)
(1)	-2.11	-2.08	0.03	1.19
(2)	-1.44	-1.55	-0.12	-8.03
(3)	-1.33	-1.38	-0.05	-3.91
(4)	-3.32	-3.03	0.29	8.78
(5)	-2.23	-1.78	0.45	20.02
(6)	-1.18	-0.34	0.84	71.01
(7)	-0.88	-0.23	0.64	73.26

Table 11(b): Comparison of vertical displacements for Case II

Model / Location	3D Beam	ISUM	Difference	
	(mm)	(mm)	(mm)	(%)
(1)	-1.72	-1.73	-0.01	-0.31
(2)	-1.13	-1.27	-0.15	-13.12
(3)	-1.03	-1.12	-0.09	-8.99
(4)	-0.60	-0.63	-0.02	-3.78
(5)	-0.56	-0.56	0.00	-0.07
(6)	-0.06	0.00	0.06	100.02
(7)	-0.06	0.00	0.06	100.01

Table 11(c): Comparison of vertical displacements for Case III

Model / Location	3D Beam	ISUM	Difference	
	(mm)	(mm)	(mm)	(%)
(1)	-0.39	-0.35	0.04	10.14
(2)	-0.31	-0.28	0.03	10.37
(3)	-0.30	-0.26	0.04	13.63
(4)	-2.60	-2.40	0.19	7.51
(5)	-1.67	-1.23	0.45	26.65
(6)	-1.11	-0.34	0.77	69.32
(7)	-0.81	-0.23	0.58	71.22

indicate that, for operations dominated by a single loading mode, the ISUM model can faithfully reproduce the structural response of the detailed model based on the effective cross-sectional area (A) and moment of inertia (I). In other words, when either axial loading or bending behavior governs the structural response, the

application of the idealized ISUM section yields results that correspond closely to those of the existing model.

In contrast, under the combined loading condition in which both column and girder loads act simultaneously (Case I), the ISUM model (**Figure 16(b)**) exhibited similar overall deformation patterns and stress distributions to those of the conventional 3D beam model (**Figure 16(a)**), but the maximum stress was approximately 20.85% lower (**Table 10**). This discrepancy is not attributable to inaccuracy in the ISUM model; rather, it suggests that the conventional 3D beam model may overestimate the member stiffness under combined loading conditions. The traditional 3D beam modeling approach simplifies each unit member as a single beam element and therefore does not fully capture the effects of non-uniform sectional properties, local stiffness variations, or realistic load redistribution within the structure. By contrast, the ISUM model derives its sectional properties by back-calculating from the structural performance of the 3D shell model, enabling a more realistic representation of stiffness distribution and stress redistribution under complex loading scenarios.

As summarized in **Table 11**, the comparison of vertical displacement responses for each loading condition shows that the maximum difference between the ISUM model and the conventional 3D beam model is less than 1.0 mm in all cases. Given the overall structural scale of the LNG cargo tank scaffolding system, such differences are negligible from a serviceability perspective. Although relatively large percentage differences were observed at certain measurement points, the absolute displacement values at those locations were very small (less than 0.1 mm). Therefore, the ISUM model is considered to provide a level of displacement response that is equivalent in reliability to that of the existing model.

4.4.3 Discussion

Based on the results of the partial model verification, the ISUM-based 1D beam model reproduces structural responses that are nearly identical to those of the conventional 3D beam model under single loading conditions, thereby confirming the appropriateness of the idealized sectional properties. In contrast, under combined loading conditions where column and girder loads act simultaneously, the results clearly reveal the potential for stiffness overestimation inherent in conventional 3D beam models. The lower stress levels predicted by the ISUM model under combined loading should not be interpreted as an underestimation of structural demand; rather, they reflect a more realistic representation of stiffness distribution and load redistribution achieved by calibrating sectional properties against reference 3D shell models. This finding indicates that conventional beam-based models may not adequately capture local stiffness variations and actual sectional behavior, whereas the proposed ISUM approach consistently reflects the effective structural performance of unit members.

Furthermore, the partial system-level analyses demonstrate that the structural performance verified at the unit-member level using the ISUM approach can be seamlessly extended to the system level without loss of consistency. This scalability highlights the potential of the proposed methodology to serve as a foundation for automated and standardized structural design and safety verification frameworks for scaffolding systems installed inside LNG cargo tanks, where geometric complexity is expected to increase in future applications.

5. Conclusion

This study proposed an Idealized Structural Unit Member-based modeling framework to enhance the efficiency and reliability of structural strength assessment for scaffolding systems installed inside LNG cargo tanks. The proposed approach replaces complex unit members composed of multiple steel components with equivalent one-dimensional beam elements whose sectional properties are calibrated against nonlinear three-dimensional shell finite element analyses.

Through systematic validation at the unit-member level, the ISUM-based model was shown to accurately reproduce both axial buckling and bending behaviors, with critical buckling loads predicted within 1% of experimental data and reference shell models. When extended to partial system-level scaffolding models, the ISUM approach demonstrated structural responses comparable to those of conventional three-dimensional beam models under single loading conditions, confirming the adequacy of the idealized sectional properties. More importantly, under combined loading conditions, the ISUM model yielded lower stress levels than conventional beam-based models, revealing the tendency of the latter to overestimate structural stiffness. This result indicates that the proposed approach provides a more physically consistent representation of stiffness distribution and load redistribution in complex scaffolding systems.

In addition to improving structural realism, the ISUM-based framework significantly reduces modeling complexity and computational cost, thereby offering clear advantages for practical design and verification workflows. The demonstrated scalability

from unit members to system-level models suggests strong potential for application to large-scale and geometrically complex scaffolding configurations inside LNG cargo tanks. Consequently, the proposed methodology provides a practical foundation for automated and standardized structural design and safety verification frameworks, and it is expected to be readily extendable to next-generation cargo containment systems with increasing structural complexity.

Acknowledgement

This work was supported by a 2-Year Research Grant of Pusan National University

Author Contributions

Conceptualization, D. Park and S. Oh; Methodology, D. Park and J.K. Seo; Resources, S. Oh and J.S. Park; Data Curation J.S. Park; Writing-Original Draft Preparation and Writing-Review & Editing, J.K. Seo; Supervision, J.K. Seo; Funding Acquisition, J.K. Seo.

References

[1] B. J. Oh, B. J. Ryu, and Y. S. Lee, “Structural and vibration characteristics for the scaffolding system of LNG Cargo containment,” Transactions of the Korean Society for Noise and Vibration Engineering, vol. 20, no. 6, pp.546-554, 2010 (in Korean).

[2] H. T. Lee, S. B. Shin, and Y. K. Park, “Development of the automatic design program for scaffolding system of the membrane LNG carrier,” Journal of the Society of Naval Architects of Korea, vol. 47, no. 2, pp. 233-241, 2010 (in Korean).

[3] S. H. Shin and D. E. Ko, “A study on 8-stage loading method of the scaffolding module for LNG carriers,” Journal of the Korea Academia-Industrial Cooperation Society, vol. 21, no.11, pp. 78-85, 2020 (in Korean).

[4] T. H. Lee, Development of scaffolding system for furnace maintenance of large supercritical power plants considering structural performance, Master's Thesis, Chungnam National University, Deajeon, 2016 (in Korean).

[5] G. M. Kim, Field application evaluation of system support using high strength steel, Ph. D. Dissertation, Cheongju University, Chungcheongbuk-do, 2020 (in Korean).

[6] J. D. Park, H. S. Lee, W. S. Shin, Y. J. Kwon, S. E. Park, S. S. Yang, and K. Jung, “Structural capacity evaluation of system scaffolding using X-type advanced guardrail,” Journal of the Korean Society of Safety, vol. 35, no. 5, pp. 49-58, 2020 (in Korean).

[7] S. N. Kim and Y. S. Roh, “An analytical study for safety check of steel pipe scaffolding - analysis of wind load and load combinations,” Journal of the Architectural Institute of Korea, vol. 39, no. 9, pp. 195-203, 2023.

[8] M. Y. Kim and S. Y. Jung, “Stability and Free Vibration of Plane Truss Structures using the Shear Flexible Beam Element,” Journal of the Korean Society of Steel Construction, vol. 8, no. 2, pp.193-203, 1996 (in Korean).

[9] I. S. Choi and I. H. Yeo, “Static and free vibration analyses of hybrid girders by the equivalent beam theory,” Journal of the Korean Society for Railway, vol. 10, no. 5, pp. 600-606, 2007.

[10] S. K. Oh, J. Park, J. K. Seo, “A simplified modelling method using idealized structural elements for conceptual design of the scaffolding system of LNG carrier cargo,” Journal of Advanced Marine Engineering and Technology, vol. 49, no.3, pp. 157-167, 2025.

[11] Japanese Industrial Standards Committee, JIS G 3444: Carbon Steel Tubes for General Structural Purposes, JIS, Tokyo, Japan, 2010.

[12] LSTC, LS-DYNA Keyword User’s Manual, Livermore Software Technology Corporation, Livermore, CA, USA, 2023.